SERBIAN JOURNAL OF ELECTRICAL ENGINEERING
Vol. 10, No. 2, June 2013, 293-307

UDK: 621.317.028.2 **DOI: 10.2298/SJEE130411005R**

An Approach to the Low-Resistance Measurement

Radojle Radetić[1], Marijana Pavlov-Kagadejev[2], Darko Brodić[3], Nikola Milivojević[4]

Abstract: The paper presents the real instrument functional characteristics and describes the way of practical solutions of its performance improvement. It presents the design process of the instrument made for resistance measuring. In order to achieve desired objectives, a great number of experiments have been carried out during the development. Basically, the comparison method has been applied. At first, it was intended for the small resistor measuring as a single range unit. Later, the device has been improved and upgraded for a wide range resistance measuring. Finally, some of the difficulties have been detected and explained as well. The paper contains solutions developed and applied for their overcoming.

Keywords: Low resistance comparator, Parasitic voltage, Measuring current, Response time.

1 Introduction

The new measuring device for testing electrical characteristics of the new materials and alloys has been designed and realized in the Laboratory of Institute for Mining and Metallurgy in Bor. The students of Bor Technical Faculty use the same laboratory and its instruments for their laboratory exercises and experimental work. The measuring unit is an electronic chopper stabilized resistance comparator, which uses a widely applied method based on comparing the voltages at the ends of two resistors [1 – 2]. It means that the ratio of resistances i.e. voltages between a standard stable, i.e. referent resistor and a test resistor are being measured.

Initially, the measuring device was designed for the low-resistance range from 10 mΩ to 100 Ω, which was divided into five sub ranges. Fig. 1 shows the realized instrument.

[1]Serbian Transmission System, Nade Dimić 40, 19210 Bor, Serbia; E-mail: radojle.radetic@ems.rs
[2]Institute for Mining and Metallurgy, Zeleni bulevar 35, 19210 Bor, Serbia;
E-mail: marijana.pavlov@irmbor.co.rs
[3]University of Belgrade, Technical Faculty in Bor, 19210 Bor, Serbia; E-mail: dbrodic@tf.bor.ac.rs
[4]University of Colorado at Boulder, 435 UCB, Boulder CO 80309-0435, USA;
E-mail: nikola.milivojevic@colorado.edu

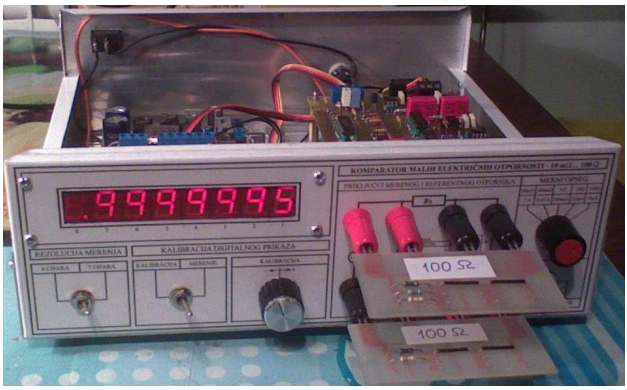

Fig. 1 – *Realized low resistance comparator.*

Its low resistance measuring mode can be briefly described by overall block diagram given in Fig. 2.

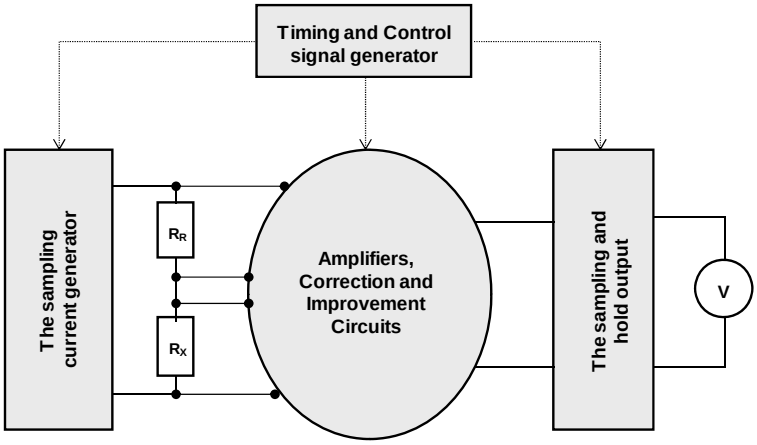

Fig. 2 – *Functional diagram of the instrument.*

The current circuit module consists of a source of measuring (sample) current, which supplies both serial connected resistors, the referent one (R_R) and unknown resistance (R_X). The same current is used through both resistors, and the voltages are amplified by the same three–stage-gain amplifier. It has been done, in order to reach the required linearity as well as to amplify both voltages in the same way. The output circuits are used to stabilize and hold the voltages until the measuring has been completed.

The control circuits generate the appropriate signals to drive the rest of electronics and to define the measuring cycles and timing. The rhythm of switching is dictated by the clock signal as in Fig. 3.

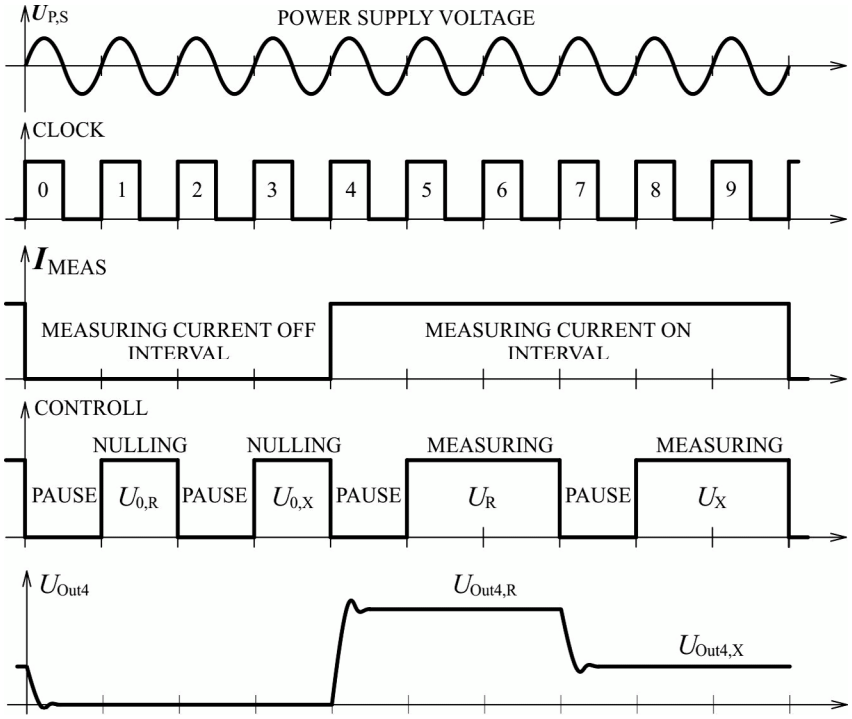

Fig. 3 – *The comparator control signals.*

The measuring cycle is divided into two periods. In the first cycle, the parasitic voltages are being measured – nulling intervals (Control signal in Fig. 3). While the measuring current is establishing, the voltage changes at the resistors terminations are being measured – measuring intervals. The result is obtained by subtraction of previously measured results and parasitic voltage values. It is known as the annulling process. In order to stabilize the voltage, the pause intervals are introduced between each nulling and measuring interval on both resistors.

Providing the same sample current through both resistors as well as using the same amplifiers to compare voltages, almost all measuring errors, occurring as the consequence due to differences of electrical circuit characteristics, can be eliminated.

The measured resistance can be calculated as the rate of voltages at the ends of resistors R_R and R_X (See Fig. 2 for the reference):

$$R_X = R_R \frac{U_X}{U_R}, \tag{1}$$

where U_X and U_R are voltages at the ends of the resistors respectively.

The above expression is simple, but in practice there are many sources of unwanted influences and disturbances, which make the measuring result worse.

Ideally, a comparator would have infinite input impedance that produces no current at the inputs. In practice, a real comparator has measurable input impedance and there is a certain amount of leakage current [3]. Parasitic DC and AC voltages are the main sources of measuring errors in chopper stabilized resistance comparator.

The practical usage of the realized instrument shows another disadvantage: too long time of showing the final i.e. correct result on the display (known as bad instrument response time). It means that the stationary state establishing sequence should be shorter. In the next chapters we will discuss those problems and the ways to overcome them.

2 The Measuring Signal Amplifying and the Parasitic Voltages influence

Good accuracy in a low-resistance measuring requires the great amplifying range and the extreme linearity as well. It is not easy to satisfy these conflicting requirements. The amplifying level could be reached by one operational amplifier (OA), but it involves a very high non-linearity [4]. That is why the amplifying chain is designed and realized as a three-stage amplifier. It is shown in Fig. 4.

In practice, the realized comparator has high, but measurable, input impedance and a certain amount of leakage current is present. These effects affect the accuracy, providing less accurate results.

Fig. 4 shows the amplifying chain. The first input amplifier, Fig. 4a is realized with two low noise operational amplifiers OP27. The amplifying range of the stage is constant, equal to 8. The second and third amplifying stages are shown in Fig. 4b. There is a total of five amplifying levels. The instrument range and amplifying rate are changing by analog switches. The amplifying rates are 8, 4 and 2 for the second, and 4 and 1 for the third level, respectively.

Considering the disturbances mentioned in previous chapter, there is the presence of the DC parasitic voltage component (for instance: thermo-voltages with value of a few tens of 1 μV and operational amplifier offset voltages), and an AC component (50 Hz) within the measured (input) voltage. Due to an intension of measuring with resolution of 0.01 μV, the impact of those effects (parasitic voltages) is too large and can considerably degrade the accuracy of resistance measurements.

The measuring process is performed in ten clock pulses [5]. A controller, based on a decade (Johnson) counter, controls all analog switches. It is driven by network supply frequency signal (50 Hz), one clock is 20 ms, and the

measuring cycle (ten clocks) takes 200 ms (Fig. 3). It provides rate of 5 measurements per second. Two of the steps are used for input parasitic voltage annulment: one for R_R and the other for R_X, the other two are used for measuring.

Design and development of the unit with fixed measuring range enable selecting the electronic component values convenient for elimination of parasitic voltages using standard correction circuit. But it is different in the case of multi-range instrument. It is necessary to apply a modified annulated electrical circuit, to eliminate all unwanted voltages in output signal, which are not the result of sample current flowing through the resistors R_R and R_X. The dominant parasitic voltage generates from operational amplifiers input voltages offset and it could reach the value of one hundred of μV.

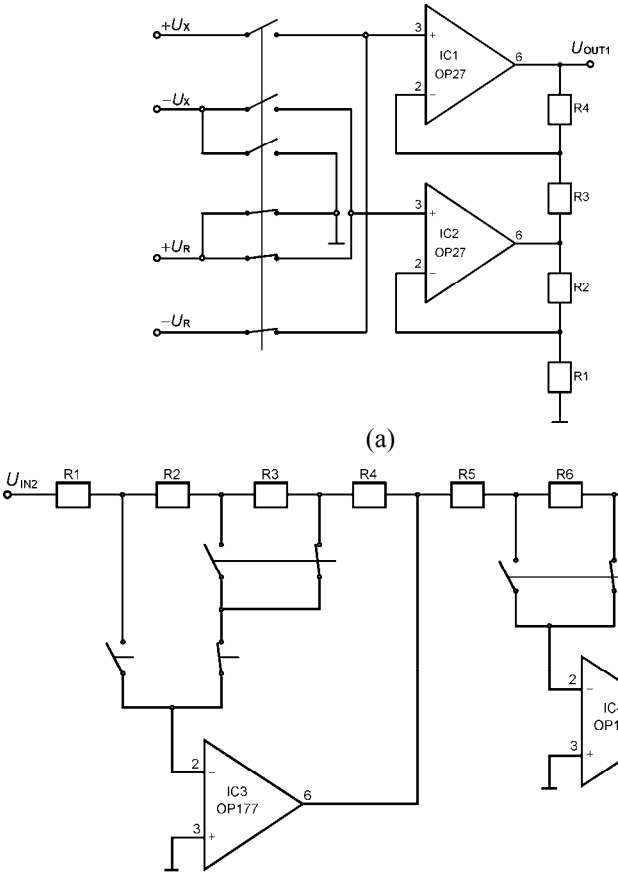

Fig. 4 – *Three-stage amplifier:* (a) *Input multiplexer with first amplifying stage,* (b) *Second and third amplifying stage*.

The DC parasitic voltage correction does not depend on controller clock frequency [6]. But the dominant role of AC disturbances has the influence on power network (50 Hz). It has turned out that the effect of that circuit, the sample and hold output circuits as well, is very much dependent on the phase difference between controller clock and network voltage frequency. That is why the controller clock is synchronized wih the network frequency.

In the case of fixed amplifying (single range mode), it is possible to overcome the problem by appropriate element selection and adjustment [1]. For the instrument with many measuring ranges, the measuring currents are different for any range as well as the amplifying rates. In that case, it is more difficult to decrease the unwanted influence of parasitic voltages [7].

To overcome the problem, the new correction circuit has been designed, Fig. 5. The new annulment circuit encircles its own offset voltages, and offset voltages of all previous amplifying stages. It operates in the following way.

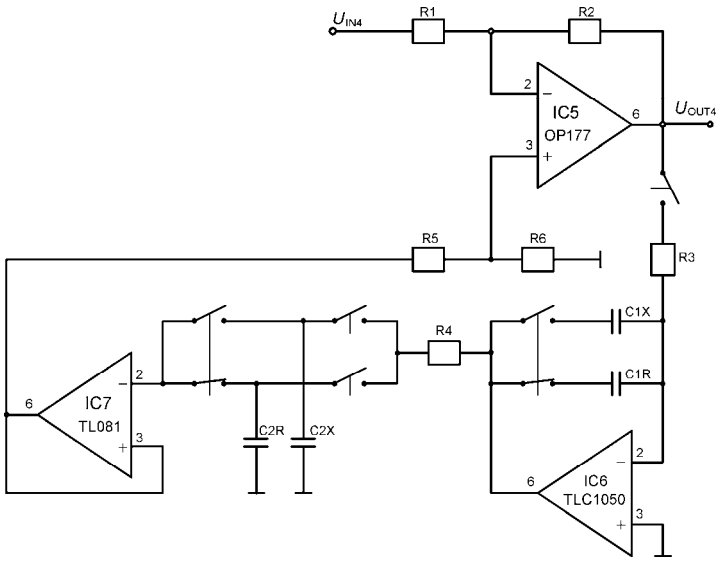

Fig. 5 – *The improved correction circuit electrical scheme*.

The necessary amplifying level has been reached in previous stages, in the way described above. The circuit of IC5 and resistors R_1 and R_2 is an output amplifier for measuring voltages signal with amplifying equal to –1. Its offset voltage is encircled by correction and it is not critical. It has to have great linearity, and an OP with very high open loop gain (over 140 dB) is in use [8]. Principle of time multiplexing allows the voltages at both resistors (referent and measured one) to be amplified by the same amplifiers. It eliminates the errors caused by difference of amplifier elements.

The same module contains the correction circuits designed to suppress many unwanted influences. The function of output circuits is to hold the clean amplified voltage until the next measuring cycle occurs. It means 0.2 s. The chopper stabilized integrated circuit IC6, together with R_3 and C_{1R} or C_{1X}, runs as an integrator and generates correction voltage. In annulling phase, the analog switch for IC6 is on and the capacitors are charging. There is no current in that period and the correction voltage at the output of IC6 equals just parasitic voltage. In the measuring interval, the switch is off and the appropriate correction voltage is led to the input of the following stage, pin 3 of IC7.

After the first step, the parasitic voltage at the IC5 output becomes significantly lower. The same process can be repeated many times to annul the parasitic voltage. Assume that it is an initial state, and the capacitor C_1 is discharged ($U_{INT0} = 0$), after the first integration period the IC5 output voltage can be expressed as:

$$U_{out1} = -\frac{1}{C_1 R_3}\int_0^T U_{out0}\,\mathrm{d}t = -\frac{U_{out0}T}{C_1 R_3}\,, \tag{2}$$

where T is the integration time (the duration of one clock period, 20 ms). This voltage has been further transferred to the capacitor C_2 by analog switches.

To reach the full capacitor charging, the time constant R_4C_2 has to be as small as possible. At the same step of measuring cycle, the equal voltage value moves to the input of IC5 amplifier (via R_5 and R_6) as a correction signal. In the following step, the value of the resultant parasitic voltage (U_{out1}) is:

$$U_{out1} = U_{out0} - \frac{U_{out0}T}{C_1 R_3}\cdot\frac{R_2}{R_1}\cdot\frac{R_6}{R_5+R_6}\,. \tag{3}$$

To prevent the fast voltage decreasing, the ratio R_5 / R_6 has to be high ($R_5 / R_6 > 100$). Now, (3) becomes:

$$U_{out1} \approx U_{out0}\left(1 - \frac{T}{C_1 R_3}\frac{R_2}{R_1}\frac{R_6}{R_5}\right) \tag{4}$$

and after k annulment steps the output voltage can be present as:

$$U_{out\,k} \approx U_{out0}\left(1 - \frac{T}{C_1 R_3}\frac{R_2}{R_1}\frac{R_6}{R_5}\right)^k\,. \tag{5}$$

The value of above expression becomes zero, if the following relation should be satisfied:

$$1 - \frac{T}{C_1 R_3}\frac{R_2}{R_1}\frac{R_6}{R_5} = 0\,. \tag{6}$$

Practically, there is a need to make more cycles to decrease the parasitic voltage to acceptable low value. It means that the electric circuit from Fig. 5 could perform fast parasitic voltages annulment, independent of voltage amplifying.

The realized circuit has shown the impressive results. In the worst case, where the lowest measuring range was 10 mΩ with amplifying rate of 256, the starting parasitic voltage was 100 mV. After first annulment cycle, it dropped below 1 mV. At the next step, it is below the scope sensitivity level.

By equalization, the controller clock duration with time period of network frequency (20 ms) and their synchronization, the integral of that disturbing voltage becomes zero and the unwanted influence of power network (AC disturbances) is eliminated [9 – 10].

3 The Measuring Current Influence

The measuring (sample) current has a significant influence on the result. If the current intensity is greater, the relative error will be lower. It is due to the higher voltage on the resistor terminals [11]. However, the stronger measuring current causes greater dissipation power and higher resistor temperature. It means that during the measuring process the resistance changes itself because of temperature influence. It makes that measuring error to be greater. Certainly, there must be the relationship between measuring current value and relative error to provide appropriate current intensity for the minimal measuring error [12]. Hence, there is a need to find optimal conditions for a minimal systematic error as a consequence of two opposite requirements. The brief analysis, one of the solutions and practical confirmation are explained below.

Considering (1), the measuring error due to limited resolution of voltage measurement ΔU_X is:

$$\Delta R_{X,(\Delta U)} = \frac{R_R}{U_R} \Delta U_X \,, \tag{7}$$

or related to:

$$\delta_U = \frac{\Delta R_X}{R_X} = \frac{\Delta U_X}{U_X} \,. \tag{8}$$

For narrow temperature intervals, the resistance variation depending on temperature can be expressed as:

$$R_X = R_{X0}(1 + \alpha \vartheta) \,, \tag{9}$$

R_{X0} – resistance at temperature ϑ_0,

α – linear resistance temperature coefficient,

$\Delta\vartheta$ – temperature increase.

In case of low power dissipation, the resistor temperature change is proportional with dissipations power and could be expressed as:

$$\Delta\vartheta = k\,P\,, \tag{10}$$

where k is the coefficient ratio (K/W).

The relationship between the resistance variation and power should be shown as:

$$R_X = R_{X0}\left(1+\alpha kP\right) = R_{X0}\left(1+\delta_P\right), \tag{11}$$

where δ_P is the resistance error as a consequence of dissipations power (self heating).

In the worst case the total measuring error obtained by (8) and (11) is:

$$\delta = \delta_U + \delta_P = \frac{\Delta U_X}{U_X} + \alpha\,k\,P\,. \tag{12}$$

The realized chopper stabilized low resistance comparator uses the switched measuring current (on and off) [1, 11]. At duty cycle (a), the power dissipation in the resistor is:

$$P = \frac{t_I}{t_I + t_P} R_X I^2 = a\,R_X I^2\,, \tag{13}$$

where:

I – current pulse intensity,

t_I – current switch on duration,

t_P – current switch off duration,

a – duty cycle (for our comparator, a = 6 / 10 = 0.6 [1, 9]).

The total measuring error could be calculated as:

$$\delta = \delta_U + \delta_P = \frac{\Delta U_X}{R_X I} + \alpha\,k\,a\,R_X I^2\,. \tag{14}$$

Equation (14) gives the relation between measuring current and total error. The shape of this relation (δ) is illustrated in Fig. 6.

Minimum value of total measuring error could be determined by:

$$\frac{\mathrm{d}\,\delta}{\mathrm{d}\,I} = -\frac{\Delta U_X}{R_X I^2} + 2\,\alpha\,k\,a\,R_X I = 0\,. \tag{15}$$

The solution gives the optimal measuring current as:

$$I_{OPT} = \sqrt[3]{\frac{\Delta U_X}{2\,\alpha\,k\,a\,R_X^2}}\,. \tag{16}$$

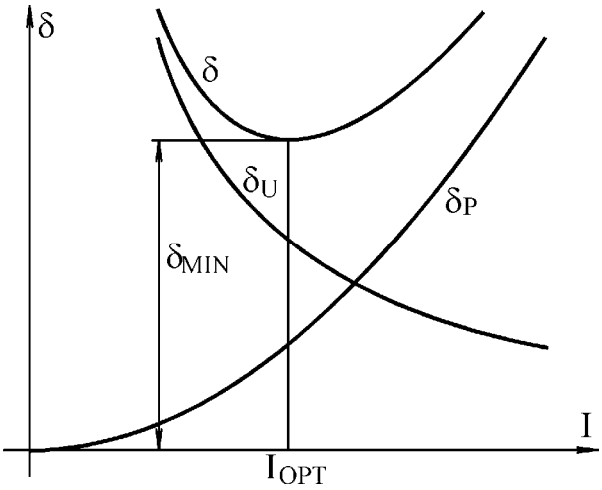

Fig. 6 – *The measuring error curves diagram.*

Using the above relation, the values of the measuring current are defined for each instrument range (See **Table 1**). For the practical instrument realization, the next parameter values were chosen as: $\alpha = 10^{-5}$ 1/K (worst case), where $k = 2.5$ K/W (for Thompson type of resistors [12]), $a = 0.6$ (projected current pulse timing) and the measuring resolution of $\Delta U_X = 10$ nV.

The measuring error is minimal with optimal current and could be calculated as:

$$\delta_{MIN} = \frac{3}{2}\sqrt[3]{\frac{2\alpha k a \Delta U_X^2}{R_X}} . \tag{17}$$

It gives the common mathematical expression for the measuring error of the chopper stabilized low resistance comparator.

$$\delta_{MIN} = \frac{3}{2}\sqrt[3]{\frac{2\cdot 10^{-5}\cdot 2.5\cdot 0.6\cdot (10^{-8})^2}{R_X}} = \frac{0.22\cdot 10^{-6}}{\sqrt[3]{R_X}} . \tag{18}$$

The equation (18) is a very useful for calculation of total systematic measurement error. Hence, the value of resistance R_X defines the instrument measuring range.

4 The Instrument Ramp-up Time

The transitional period is the time interval between the switching on the instrument (measuring start) and the moment when the result has been shown. Sometimes it is called rump-up time, or stationary state establishing [3]. The instrument measuring cycle includes 10 steps (See Fig. 3 for reference). The

time of presence for both input voltages (U_R and U_X) is 40 ms each, followed by 160 ms of pause [9 – 10].

Because of capacitor discharging in a time and as a consequence of current leaking occurring, the measuring voltage is decreasing during the measuring time. To make the voltage changes as small as possible during that period, the great capacitor is needed. In the original solution (See Fig. 1 for reference), the high input resistance is used to decrease the AC disturbances. But, those conditions give the great time constant, and the time to achieve stationary state becomes longer. The charge injection effect makes the instrument performances worse, too [11]. The long instrument response time could be considered as its consequence as well. To overcome the problems, the redesign of output voltage hold circuit has been done. It is shown in Fig. 7.

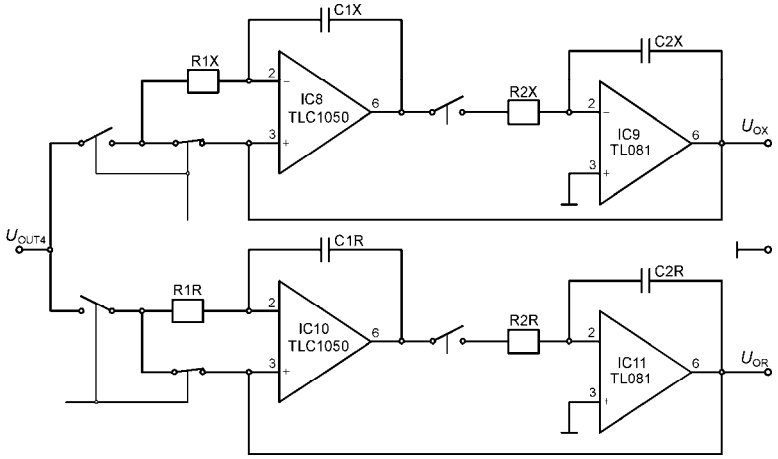

Fig. 7 – *The output demultiplexer and new output circuit.*

The modified circuit operates in the following way: At the very beginning the capacitors are discharged (initial state). In the first measuring interval, the output voltage of IC8 equals the IC9 offset voltage, $U_{offset2}$, Fig. 7. At the end of integration time period the input voltage at capacitor C_1[5] reaches value of:

$$U_{\text{int}1} = -\frac{1}{R_1 C_1}\int_0^{2T}(U_{IN} - U_{offset2})\,\mathrm{d}t = -\frac{2T}{R_1 C_1}(U_{IN} - U_{offset2}), \qquad (19)$$

where $T = 20$ ms is an integration period (one clock of measuring cycle, see Fig. 3) [7].

After integration has finished, the switches change their own states. At that period, the second OA runs as an integrator and raises its voltage. It is valid

[5]The symbols R_1 and C_1 are used as a common sign for both input voltages: U_R and U_X.

until the output voltage of first integrator becomes equal to the input offset voltage of the second one, $U_{offset2}$. At that time, the output voltage of the second integrator equals $-U_{out1}$.

$$U_{out1} = -U_{\text{int}1} + U_{offset2} \,. \tag{20}$$

Equations (19) and (20) give the following:

$$U_{Out1} = \frac{2T}{R_1 C_1} U_{IN} + (1 - \frac{2T}{R_1 C_1}) U_{offset2} \,. \tag{21}$$

If the resistor and capacitor values satisfy the equation $R_1C_1 = 2T$, then (21) becomes:

$$U_{Out1} = U_{IN} \,. \tag{22}$$

That is an ideal case. The stationary state is established after first measuring cycle. The small deviation of necessary condition ($R_1C_1 = 2T$) requires a few more steps in order to reach the operational mode.

Using the scope for the ramp-up time shows disadvantage because all of the parameters reach their right values in the first annulment cycle. Hence, the transition could not be visible at the screen. That is the reason why the simulation was done with the different component values. In annulment circuits (Fig. 4), the value of resistor R_6 is chosen 20% higher than optimal. The value of resistor R_1 in hold circuit (Fig. 5) needs a similar approach. It is assumed that the input voltage in annulment circuit contains the DC and AC voltages of 10 mV both (U_{IN} = 10 mV_{DC} + 10 mV_{AC}). Accordingly, the simulation result is shown in Fig. 8.

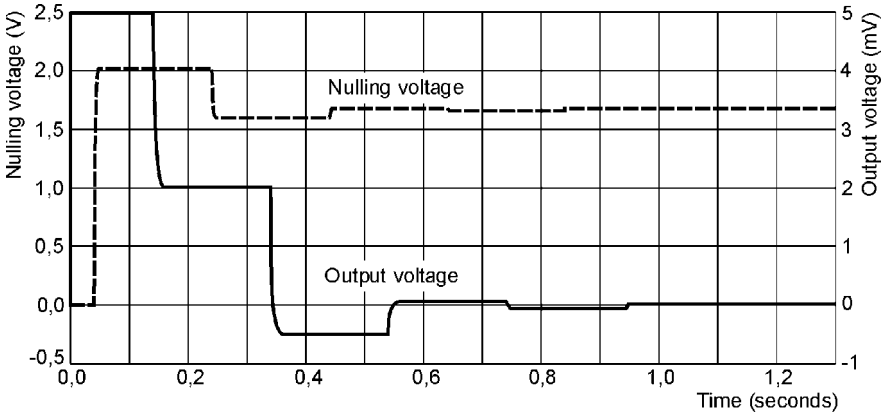

Fig. 8 – *The ramp-up diagram*.

In Fig. 8, the upper line (Nulling voltage) represents the annulment voltage (circuit IC7 output) while the bottom curve (Output voltage) shows IC9 circuit

output voltage. It is easy to note that with those parameter values the output voltage drops below 10 mV for a time shorter than 1 s. It is quite acceptable for the instrument response time.

5 The Comment of Practical Results

It should be noted that some of the instrument measuring errors are not possible to nullify at all. For example: the capacitor self discharging in output hold circuits, output operational amplifiers drift and offset voltages and uncertainty in the switching of the comparator [10]. But, the proposed circuits are good enough as the caused errors are rather small, reduced to acceptable level, i.e. less than 1 ppm [12].

The error sources like:

– parasitic voltages,

– measuring output voltage instability,

– measuring current influence,

– and long ramp-up time

have been decreased as much as possible. The analog switch charge injection and similar ones are successfully overcome by the proposed solutions. Considering all of the occurred problems and using the proposed solutions, the realized measuring unit [1] reaches good performances [5, 14 – 15] which are given in **Table 1**.

Table 1

The practical conformed main instrument characteristics for small resistances.

Measuring Range [Ω]	0.01	0.1	1	10	100
Measuring Current [A]	2	0.4	0.08	0.016	0.0032
Voltage gain	256	128	64	32	16
Resolution [ppm]	5	1	1	1	1

6 Conclusion

The instrument functional characteristics have been described in this paper. There have been notice some disadvantages in practical design and realization. Few efficient solutions for their overcoming and performance improvement have been presented. However, many of the problems occurred by upgrading the prototype of a single range instrument for usage in different resistance ranges. Applying the explained solutions, the initial goal is achieved: the unit becomes a multi-range instrument by noncomplex modification and extension

without high costs. The realized instrument has shown impressive results: in the worst case (the lowest measuring range of 10 mΩ and amplifying of 256) the starting parasitic voltage was 100 mV. After first annulment cycle it drops below 1 mV and at the next step, below the scope sensitivity level. The stationary state establishing is significantly shortened. The influence of DC and AC disturbances is decreased at the acceptable level [16]. Based on described solution, the realized comparator reaches measuring resolution of 1 ppm in the range of 0.01 Ω to 100 Ω for small resistances (See **Table 1** for reference).

At the moment, the realized instrument (See Fig. 1 for reference) is working as a prototype in a laboratory at Mining and Metallurgy Institute in Bor. There is an intention of integrating it into standard operative laboratory equipment for electrical measuring and for a new materials resistance and conductivity measurement. The student laboratory exercises at the Bor Technical Faculty require the wide range of resistance to be measured as well. Furthermore, the automatic instrument with PC connection would be very welcome. Hence, the authors intend to upgrade the instrument in that direction.

7 Acknowledgment

This paper is supported by the Grant of the Ministry of Science of Republic of Serbia, as a part of the projects: *Development and application of distributed system for monitoring and control of electrical energy consumption of large consumers* – TR33037 and *Development of ecological knowledge-based advanced materials and technologies for multifunctional application* – TR 34005, within the framework of Technological development program.

7 References

[1] R. Radetic: Low Resistance Electronic Comparator, PhD Thesis, Faculty of Technical Sciences, University of Novi Sad, Novi Sad, Serbia, 2009. (In Serbian)

[2] B.P. Kibble, D.J. Legg: A Generalized Wheatstone Bridge for Comparing 1-Ω Resistors, IEEE Transaction on Instrumentation and Measurement, Vol. 34, No. 2, June 1985, pp. 282 – 284.

[3] V.S. Aleksandrov, N.N. Trunov, A.A. Lobashev: General Problems of Metrology and Measurement Technique System Approach to Metrology of Quantum Multiparticle Systems, Measurement Techniques, Vol. 51, No. 4, April 2008. pp. 345-350.

[4] H. Ercan, S.A. Tekin, M. Alci: Voltage- and Current-controlled High CMRR Instrumentation Amplifier using CMOS Current Conveyors, Turkish Journal of Electrical Engineering and Computer Sciences, Vol. 20, No. 4, July 2012, pp. 547 – 556.

[5] http://www.ti.com/lit/an/slva450/slva450.pdf.

[6] G.C. Barney: Intelligent Instrumentation: Microprocessor Applications in Measurement and Control, Prentice Hall, London, UK, 1988.

[7] H.N. Norton: Handbook of Transducers, Prentice Hall, Englewood Cliffs, NJ, USA, 1998.

[8] Wavetek Corporation, Wawetek, Model 1281/1271 Data Sheet, 1997.

[9] R.M. Radetic, D.R. Milivojevic: Chopper Stabilized Low Resistance Comparator, Sensors, Vol. 9, No. 4, April 2009, pp. 2491 – 2497.

[10] R.M. Radetic, D.R. Milivojevic, M. Pavlov: The New Bridge Converter Control Method, Measurement Science Review, Vol. 10, No. 1, Feb. 2010, pp. 25 – 27.

[11] R.M. Radetic, D.R. Milivojevic, V.M. Despotovic: Optimization of Measuring Current for Chopper Low Resistance Comparator, Measurement Science Review, Vol. 10, No. 1, Feb. 2010, pp. 22 – 24.

[12] Understanding Dielectric Absorption (105), SENCORE, Sioux Falls, SD, USA. Available at: www.sencore.com.

[13] V.V. Vitorov, F.I. Kharapov: Processing the Result of a Check of Measuring Instruments using Stable Methods of Parameter Estimation, Measurement Techniques, Vol. 51, No. 4, April 2008, pp. 366 – 369.

[14] B. Nuckolls: Practical Low Resistance Measurements, The AeroElectric Connection, 2004.

[15] Keithley Instruments Inc. 8½-digit Digital Multimeters Data Sheet, 2002.

[16] R. Radetic, D.R. Milivojevic, M. Pavlov: The Low Resistance Comparator Performances Improvement, 16th International Symposium on Power Electronics, 26 – 28 Oct. 2011, Novi Sad, Serbia, Paper No. T4-1.4.